ICCC 2004

2004 International Conference on Computational Cybernetics

Proceedings

Vienna, Austria - August 30 - September 1, 2004

Hungarian Fuzzy Association

Budapest Tech, Hungary

Vienna University of Technology, Austria

IEEE SMC Chapter, Hungary

IEEE NN Chapter, Hungary

IEEE Joint Chapter of IES and RAS, Hungary

IEEE R8

IEEE Systems, Man, and Cybernetics Society

EUROFUSE

Japan Society for Fuzzy Theory and Intelligent Informatics

John von Neumann Computer Society, Budapest, Hungary

IEEE

Gait Selection for Quadruped and Hexapod Walking Systems

Manuel F. Silva, J. A. Tenreiro Machado
Dept. of Electrical Engineering
Institute of Engineering of Porto
Rua Dr. António Bernardino de Almeida
4200-072 Porto, Portugal
{mfsilva,jtm}@dee.isep.ipp.pt

António M. Lopes
Dept. of Mechanical Engineering
Faculty of Engineering of Porto
Rua Dr. Roberto Frias
4200-465 Porto, Portugal
aml@fe.up.pt

József K. Tar
Inst. of Math. and Comp. Sciences
Budapest Polytechnic
Népszínház utca 8.
H-1081 Budapest, Hungary
tar.jozsef@nik.bmf.hu

Abstract — **This paper studies periodic gaits of quadruped and hexapod locomotion systems. The purpose is to determine the best set of gait and locomotion variables for different robot velocities based on the system dynamics during walking. In this perspective, several performance measures are formulated and a set of experiments that reveal the influence of the gait and locomotion variables upon those proposed indices are performed.**

I. INTRODUCTION

Walking machines allow locomotion in terrain inaccessible to other type of vehicles, since they do not need a continuous support surface. On the other hand, the requirements for leg coordination and control impose difficulties beyond those encountered in wheeled robots [1]. Gait analysis and selection is a research area requiring an appreciable modeling effort for the improvement of mobility with legs in unstructured environments [2 – 6]. Previous studies mainly focused in the structure and selection of locomotion modes. Nevertheless, there are different optimization criteria such as energy efficiency [3], stability [4], velocity [5], mobility [6], comfort and environmental impact. In this line of thought, a simulation model for multi-leg locomotion systems was developed, for several periodic gaits [1, 7]. This study intends to generalize previous work [8 – 9] through the formulation of several indices measuring the system dynamics and the hip trajectory errors during forward straight line walking at different velocities.

Bearing these facts in mind, the paper is organized as follows. Section two introduces the robot kinematic model and the motion planning scheme. Sections three and four present the robot dynamic model and control architecture and the optimizing indices, respectively. Section five develops a set of experiments that reveal the influence of the locomotion parameters and robot gaits on the performance measures, as a function of robot body velocity. Finally, section six outlines the main conclusions.

II. KINEMATICS AND TRAJECTORY PLANNING

We consider a walking system (Fig. 1) with n legs ($n = \{4, 6\} \equiv \{\text{quadruped, hexapod}\}$), equally distributed along both sides of the robot body, having each two rotational joints (*i.e.*, $j = \{1, 2\} \equiv \{\text{hip, knee}\}$).

Motion is described by means of a world coordinate system. The kinematic model comprises: the cycle time T, the duty factor β, the transference time $t_T = (1-\beta)T$, the support time $t_S = \beta T$, the step length L_S, the stroke pitch S_P, the body height H_B, the maximum foot clearance F_C, the i^{th} leg lengths L_{i1} and L_{i2} and the foot trajectory offset O_i ($i = 1, \ldots, n$). Moreover, we consider a periodic trajectory for each foot, with body velocity $V_F = L_S / T$.

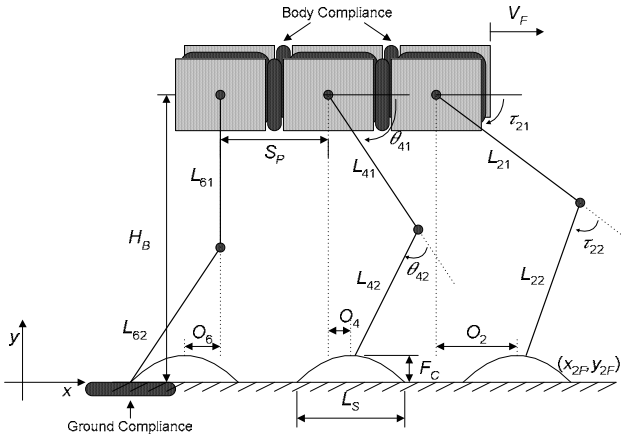

Fig. 1. Kinematic and dynamic multi-legged robot model

Gaits describe sequences of leg movements, alternating between transfer and support phases. Given a particular gait and duty factor β, it is possible to calculate, for leg i, the corresponding phase ϕ_i, the time instant where each leg leaves and returns to contact with the ground and the cartesian trajectories of the tip of the feet (that must be completed during t_T) [1]. Based on this data, the trajectory generator is responsible for producing a motion that synchronises and coordinates the legs.

The robot body, and by consequence the legs hips, is assumed to have a desired horizontal movement with a constant forward speed V_F. Therefore, for leg i the cartesian coordinates of the hip of the legs are given by $\mathbf{p_{Hd}}(t) = [x_{iHd}(t), y_{iHd}(t)]^{\mathrm{T}}$:

$$\mathbf{p_{Hd}}(t) = \begin{bmatrix} V_F t & H_B \end{bmatrix}^{\mathrm{T}} \tag{1}$$

Regarding the feet trajectories, on a previous work we evaluated two alternative space-time foot trajectories, namely a cycloidal and a sinusoidal function [10]. It was demonstrated that the cycloid is superior, because it improves the hip and foot trajectory tracking, while minimising the corresponding joint torques. For different acceleration profiles of the foot trajectory there were no significant changes of these results.

Considering these results, for each cycle the desired trajectory of the foot of the swing leg is computed through a cycloid function (Eq. 2). For example, considering that the transfer phase starts at $t = 0$ for leg $i = 1$ we have for $\mathbf{p_{Fd}}(t) = [x_{iFd}(t), y_{iFd}(t)]^{\mathrm{T}}$:

- during the transfer phase:

$$\mathbf{p_{Fd}}(t) = \left[V_F \left[t - \frac{T}{2\pi} \sin\left(\frac{2\pi t}{T} \right) \right], \quad \frac{F_C}{2} \left[1 - \cos\left(\frac{2\pi t}{T} \right) \right] \right]^{\mathrm{T}} \tag{2}$$

- during the stance phase:

$$\mathbf{p_{Fd}}(t) = \begin{bmatrix} V_F T & 0 \end{bmatrix}^{\mathrm{T}} \tag{3}$$

The algorithm for the forward motion planning accepts the desired cartesian trajectories of the leg hips $\mathbf{p_{Hd}}(t)$ and feet $\mathbf{p_{Fd}}(t)$ as inputs and, by means of an inverse kinematics algorithm $\boldsymbol{\psi}^{-1}$, generates the related joint trajectories $\boldsymbol{\Theta}_\mathbf{d}(t) = [\theta_{i1d}(t), \theta_{i2d}(t)]^{\mathrm{T}}$, selecting the solution corresponding to a forward knee:

$$\mathbf{p_d}(t) = \begin{bmatrix} x_{id}(t) & y_{id}(t) \end{bmatrix}^{\mathrm{T}} = \mathbf{p_{Hd}}(t) - \mathbf{p_{Fd}}(t) \tag{4a}$$

$$\mathbf{p_d}(t) = \boldsymbol{\psi}[\boldsymbol{\Theta}_\mathbf{d}(t)] \Rightarrow \boldsymbol{\Theta}_\mathbf{d}(t) = \boldsymbol{\psi}^{-1}[\mathbf{p_d}(t)] \tag{4b}$$

$$\dot{\boldsymbol{\Theta}}_\mathbf{d}(t) = \mathbf{J}^{-1}[\dot{\mathbf{p}}_\mathbf{d}(t)],\ \mathbf{J} = \frac{\partial \boldsymbol{\psi}}{\partial \boldsymbol{\Theta}} \tag{4c}$$

In order to avoid the impact and friction effects, at the planning phase we estimate null velocities of the feet in the instants of landing and taking off, assuring also the velocity continuity.

III. DYNAMICS AND CONTROL ARCHITECTURE

A. Inverse Dynamics Computation

The planned joint trajectories constitute the reference for the robot control system. The model for the robot inverse dynamics is formulated as:

$$\boldsymbol{\Gamma} = \mathbf{H}(\boldsymbol{\Theta})\ddot{\boldsymbol{\Theta}} + \mathbf{c}(\boldsymbol{\Theta}, \dot{\boldsymbol{\Theta}}) + \mathbf{g}(\boldsymbol{\Theta}) - \mathbf{F_{RH}} - \mathbf{J_F^T}(\boldsymbol{\Theta})\mathbf{F_{RF}} \tag{5}$$

where $\boldsymbol{\Gamma} = [f_{ix}, f_{iy}, \tau_{i1}, \tau_{i2}]^{\mathrm{T}}$ ($i = 1, \ldots, n$) is the vector of forces/torques, $\boldsymbol{\Theta} = [x_{iH}, y_{iH}, \theta_{i1}, \theta_{i2}]^{\mathrm{T}}$ is the vector of position coordinates, $\mathbf{H}(\boldsymbol{\Theta})$ is the inertia matrix and $\mathbf{c}(\boldsymbol{\Theta}, \dot{\boldsymbol{\Theta}})$ and $\mathbf{g}(\boldsymbol{\Theta})$ are the vectors of centrifugal/Coriolis and gravitational forces/torques, respectively. The $n \times m$ ($m = 2$) matrix $\mathbf{J_F^T}(\boldsymbol{\Theta})$ is the transpose of the robot Jacobian matrix, $\mathbf{F_{RH}}$ is the $m \times 1$ vector of the body inter-segment forces and $\mathbf{F_{RF}}$ is the $m \times 1$ vector of the reaction forces that the ground exerts on the robot feet. These forces are null during the foot transfer phase.

Furthermore, we consider that the joint actuators are not ideal, exhibiting a saturation given by:

$$\tau_{ijm} = \begin{cases} \tau_{ijC}, & |\tau_{ijm}| \le \tau_{ijMax} \\ \mathrm{sgn}(\tau_{ijC}) \cdot \tau_{ijMax}, & |\tau_{ijm}| > \tau_{ijMax} \end{cases} \tag{6}$$

where, for leg i and joint j, τ_{ijC} is the controller demanded torque, τ_{ijMax} is the maximum torque that the actuator can supply and τ_{ijm} is the motor effective torque.

B. Robot Body Model

Figure 1 presents the dynamic model for the hexapod body and foot-ground interaction. It is considered a robot body compliance because walking animals have a spine that allows supporting the locomotion with improved stability. In the present study, the robot body is divided in n identical segments (each with mass $M_b n^{-1}$) and a linear spring-damper system is adopted to implement the intra-body compliance according to:

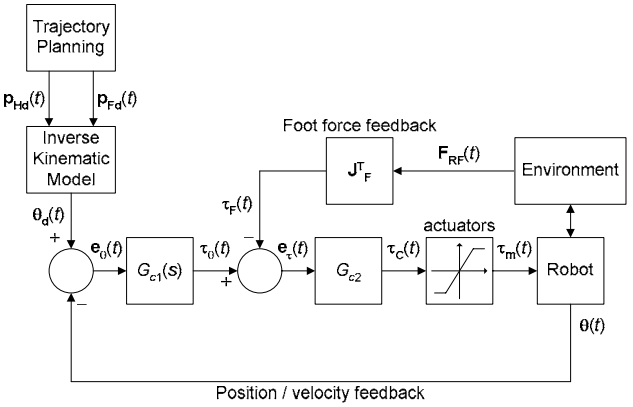

Fig. 2. Multi-legged robot control architecture

$$f_{ixH} = \sum_{i'=1}^{u} \left(-K_{xH} \Delta_{i'xH} - B_{xH} \dot{\Delta}_{i'xH} \right) \tag{7a}$$
$$\Delta_{i'xH} = x_{iH} - x_{i'H},\ \dot{\Delta}_{i'xH} = \dot{x}_{iH} - \dot{x}_{i'H}$$

$$f_{iyH} = \sum_{i'=1}^{u} \left(-K_{yH} \Delta_{i'yH} - B_{yH} \dot{\Delta}_{i'yH} \right) \tag{7b}$$
$$\Delta_{i'yH} = y_{iH} - y_{i'H},\ \dot{\Delta}_{i'yH} = \dot{y}_{iH} - \dot{y}_{i'H}$$

where $(x_{i'H}, y_{i'H})$ are the hip coordinates and u is the total number of segments adjacent to leg i, respectively. In this study, the parameters $K_{\eta H}$ and $B_{\eta H}$ ($\eta = \{x, y\}$) in the {horizontal, vertical} directions, respectively, are defined so that the body behaviour is similar to the one expected to occur on an animal (Table I).

C. Foot-Ground Interaction Model

The contact of the i^{th} robot foot with the ground is modeled through a non-linear system [10] with a linear stiffness $K_{\eta F}$ and a non-linear damping $B_{\eta F}$ ($\eta = \{x, y\}$) in the {horizontal, vertical} directions, respectively (see Fig. 1), yielding:

$$f_{ixF} = -K_{xF} \Delta_{ixF} - B_{xF} \left(-\Delta_{iyF} \right) \dot{\Delta}_{ixF} \tag{8a}$$
$$\Delta_{ixF} = x_{iF} - x_{iF0},\ \dot{\Delta}_{ixF} = \dot{x}_{iF} - \dot{x}_{iF0}$$

$$f_{iyF} = -K_{yF} \Delta_{iyF} - B_{yF} \left(-\Delta_{iyF} \right)^{v} \dot{\Delta}_{iyF} \tag{8b}$$
$$\Delta_{iyF} = y_{iF} - y_{iF0},\ \dot{\Delta}_{iyF} = \dot{y}_{iF} - \dot{y}_{iF0}$$

where x_{iF0} and y_{iF0} are the coordinates of foot i touchdown and v is a parameter dependent on the ground characteristics. The values for the parameters $K_{\eta F}$ and $B_{\eta F}$ (Table I) are based on the studies of soil mechanics [10].

D. Control Architecture

The general control architecture of the multi-legged locomotion system is presented in Fig. 2. The trajectory planning is held at the cartesian space but the control is performed in the joint space, which requires the integration of the inverse kinematic model in the forward path. The control algorithm considers an external position and velocity feedback and an internal feedback loop with information of foot-ground interaction force.

On a previous work it was demonstrated the superior performance of introducing force feedback and this was highlighted for the case of having non-ideal actuators with saturation or variable ground characteristics [10].

Based on these results, in this study we adopt a *PD* controller for $G_{c1}(s)$ and a simple *P* controller for G_{c2}, with gain $Kp_j = 0.9$. For the *PD* algorithm we have:

$$G_{C1j}(s) = Kp_j + Kd_j s, \quad j = 1,2 \tag{9}$$

where Kp_j and Kd_j are the proportional and derivative gains.

IV. MEASURES FOR PERFORMANCE EVALUATION

In mathematical terms we establish several global measures of the overall mechanism performance in an average sense [8 – 9]. In this perspective, we define three indices $\{E_{av}, D_{av}, T_L\}$ inspired on the system dynamics and one index $\{\varepsilon_{xyH}\}$ based on the trajectory tracking errors.

A first measure in this analysis is the mean absolute density of energy per travelled distance E_{av}. This index is computed assuming that energy regeneration is not available by actuators doing negative work, that is, by taking the absolute value of the power. At a given joint *j* and leg *i*, the mechanical power is the product of the motor torque and angular velocity. The global index E_{av} is obtained by averaging the mechanical absolute energy delivered over the travelled distance *L*:

$$E_{av} = \frac{1}{L}\sum_{i=1}^{n}\sum_{j=1}^{m}\int_0^T \left|\boldsymbol{\tau}_{ijm}(t)\dot{\boldsymbol{\theta}}_{ij}(t)\right| dt \tag{10}$$

Although minimising energy appears to be an important consideration, it may occur instantaneous, very high, power demands. In such cases, the average value can be small while the peaks are physically unrealisable. An alternative index is the standard deviation per meter that evaluates the dispersion around the mean absolute energy over a complete cycle *T* and travelled distance *L*:

$$P_i(t) = \sum_{i=1}^{n}\sum_{j=1}^{m}\left|\boldsymbol{\tau}_{ijm}(t)\dot{\boldsymbol{\theta}}_{ij}(t)\right| \tag{11a}$$

$$D_{av} = \frac{1}{L}\sqrt{\frac{1}{T}\int_0^T \left[P_i(t) - E_{av}/T\right]^2 dt} \tag{11b}$$

where P_i is the total instantaneous absolute mechanical power.

A third measure consists on T_L, the density of power lost in the joint actuators per travelled distance *L*, that is:

$$T_L = \frac{1}{L}\sqrt{\frac{1}{T}\sum_{i=1}^{n}\sum_{j=1}^{m}\int_0^T \left[\boldsymbol{\tau}_{ijm}(t)\right]^2 dt} \tag{12}$$

In what concerns the hip trajectory following errors we can define the index:

$$\varepsilon_{xyH} = \sum_{i=1}^{n}\sqrt{\frac{1}{N_S}\sum_{k=1}^{N_S}\left(\Delta_{ixH}{}^2 + \Delta_{iyH}{}^2\right)}, \tag{13}$$

$$\Delta_{ixH} = x_H^d(k) - x_H^r(k), \quad \Delta_{iyH} = y_H^d(k) - y_H^r(k)$$

TABLE I

SYSTEM PARAMETERS

Robot model parameters		**Locomotion parameters**	
S_P	1 m	L_S	1 m
L_{ij}	0.5 m	H_B	0.9 m
O_i	0 m	F_C	0.1 m
M_b	88.0 kg	**Ground parameters**	
M_{ij}	1 kg	K_{xF}	1302152.0 Nm^{-1}
K_{xH}	10^5 Nm^{-1}	K_{yF}	1705199.0 Nm^{-1}
K_{yH}	10^4 Nm^{-1}	B_{xF}	2364932.0 Nsm^{-1}
B_{xH}	10^3 Nsm^{-1}	B_{yF}	2706233.0 Nsm^{-1}
B_{yH}	10^2 Nsm^{-1}	v	0.9

where N_S is the total number of samples for averaging purposes and $\{d, r\}$ indicate the i^{th} samples of the desired and real position, respectively.

In all cases the performance optimization requires the minimization of each index.

V. SIMULATION RESULTS

To illustrate the use of the preceding concepts, in this section we develop a set of simulation experiments to estimate the influence of parameters β, L_S and H_B, when adopting periodic gaits.

In a first phase, we study an hexapod adopting the *WG* and then examine the variation of the performance indices with other gaits, for different controller tunings. Afterwards, an identical analysis is developed for a quadruped robot.

In a second phase, we implement several walking patterns commonly found in nature for quadrupeds. The quadruped robot is then simulated in order to compare the performance of the different gaits *versus* V_F, for different controller tunings.

In both phases the robot is controlled through a *PD* joint leg controller. With this algorithm, large forces occur during the feet impact with the ground, giving rise to torques that propagate through the leg mechanical structure up to the joints. In order to determine the impact influence upon the results, the experiments are repeated for an ideal case where we have the planned robot trajectories.

In all simulations, the discrete-time control algorithm is evaluated with a sampling frequency of f_{sc} = 2.0 kHz while the robot and environment dynamics are calculated with a sampling frequency of f_{sr} = 20.0 kHz.

A. Controller Tuning Methodology

For the system simulation we consider the robot body parameters, the locomotion parameters and the ground parameters presented in Table I. Moreover, we assume high performance joint actuators with a maximum torque in (6) of τ_{ijMax} = 400 Nm.

To tune the controller we adopt a systematic method, testing and evaluating a grid of several possible combinations of controller parameters, while establishing a compromise in what concerns the minimisation of E_{av} (10) and ε_{xyH} (13).

TABLE II

HEXAPOD CONTROLLER PARAMETERS

	$V_F = 0.2$ ms^{-1}		$V_F = 1.0$ ms^{-1}		$V_F = 5.0$ms^{-1}	
$\beta = 25\%$	Kp_1	8000	Kp_1	10000	Kp_1	200
	Kd_1	0	Kd_1	40	Kd_1	100
	Kp_2	500	Kp_2	500	Kp_2	2000
	Kd_2	60	Kd_2	20	Kd_2	60
$\beta = 50\%$	Kp_1	9000	Kp_1	1000	Kp_1	700
	Kd_1	120	Kd_1	180	Kd_1	100
	Kp_2	5000	Kp_2	2500	Kp_2	7500
	Kd_2	0	Kd_2	40	Kd_2	10
$\beta = 75\%$	Kp_1	7000	Kp_1	4000	Kp_1	7500
	Kd_1	140	Kd_1	180	Kd_1	60
	Kp_2	4000	Kp_2	3500	Kp_2	200
	Kd_2	20	Kd_2	20	Kd_2	10

B. Locomotion Parameters versus Body Forward Velocity

In order to analyse the evolution of the locomotion parameters β, L_S and H_B with V_F, for a given gait, the robot controller is tuned for different values of the forward velocity $V_F = \{0.2\ \text{ms}^{-1}, 1.0\ \text{ms}^{-1}, 5.0\text{ms}^{-1}\}$ and duty factor $\beta = \{25\%, 50\%, 75\%\}$, while adopting the *WG*, resulting the possible controller parameters presented in Table II.

After completing the controller tuning, the robot forward straight line locomotion is simulated for different gaits, while varying the body velocity on the range $0.2 \le V_F \le 4.0\ \text{ms}^{-1}$. In the simulations, we consider the gaits {Wave, Equal Phase Half Cycle, Equal Phase Full Cycle, Backward Wave, Backward Equal Phase Half Cycle, Backward Equal Phase Full Cycle} ≡ {*WG*, *EPHC*, *EPFC*, *BW*, *BEPHC*, *BEPFC*} [1]. For each gait and body velocity, the set of locomotion parameters (β, L_S, H_B) that minimises a given optimization index is determined.

The charts presented in Fig. 3 depict the minimum value of the index E_{av}, on the range of V_F under consideration, for three different robot joint leg controller tunings. It is possible to conclude that the minimum values of the index E_{av} increase with V_F, independently of the adopted controller tuning. Although not presented here, due to space limitations, the behaviour of the charts min[$E_{av}(V_F)$], for all other controller tunings present similar shapes. This increase with V_F is observed on the other performance indices, irrespectively of the controller tuning adopted, as can be seen in the chart of Fig. 4 for the case of D_{av}.

Next we analyse how the locomotion parameters vary with V_F. Figures 5 and 6 show that the optimal value of β decreases with V_F, while analysing the robot locomotion through the indices E_{av} and T_L, respectively. Moreover, Fig. 7 reveals that the optimal value of L_S must increase with V_F when considering the performance index E_{av}. Finally, Fig. 8 shows that H_B must decrease with V_F from the viewpoint of the performance index T_L.

The variations of the three locomotion parameters (β, L_S, H_B) are similar when analysing the robot locomotion through the other performance indices and for the different robot joint leg controller tunings under consideration (Table II).

For the other periodic walking gaits considered on this study, the evolution of the optimization indices and the locomotion parameters with V_F follows the same pattern.

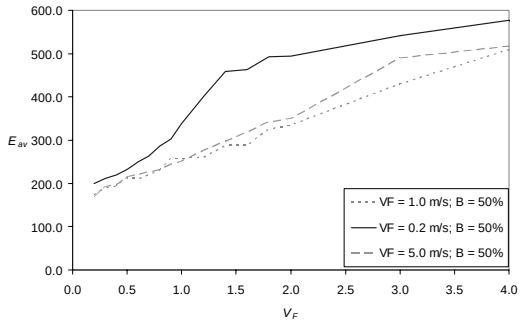

Fig. 3. Plots of min[$E_{av}(V_F)$] for F_C = 0.1 m, *WG*

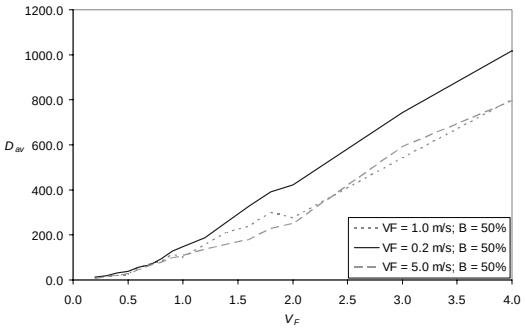

Fig. 4. Plots of min[$D_{av}(V_F)$] for F_C = 0.1 m, *WG*

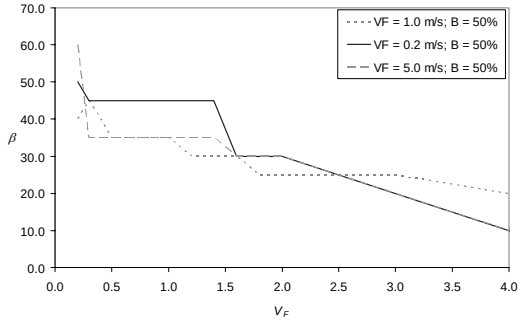

Fig. 5. Plots of $\beta(V_F)$ for min(E_{av}) with F_C = 0.1 m, *WG*

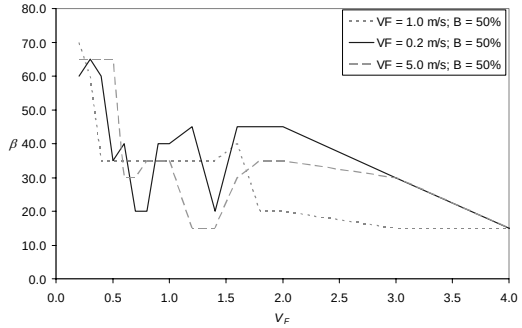

Fig. 6. Plots of $\beta(V_F)$ for min(T_L) with F_C = 0.1 m, *WG*

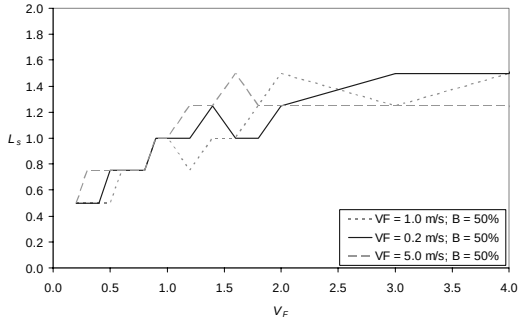

Fig. 7. Plots of $L_S(V_F)$ for min(E_{av}) with F_C = 0.1 m, *WG*

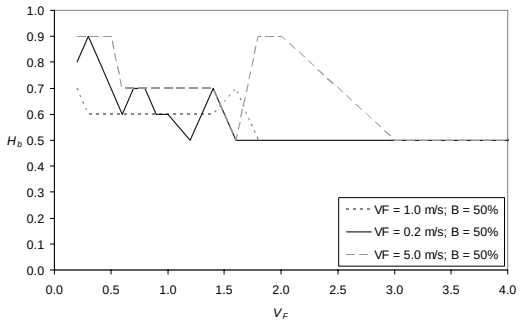

Fig. 8. Plots of $H_B(V_F)$ for min(T_L) with F_C = 0.1 m, *WG*

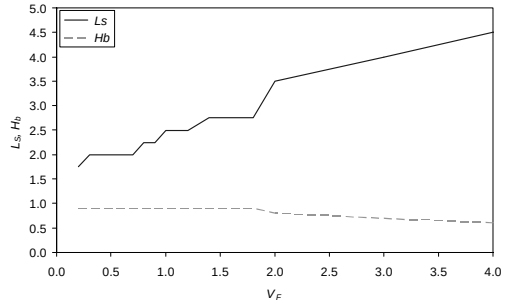

Fig. 9. Plots of $L_S(V_F)$ and $H_B(V_F)$ for min(E_{av}) with F_C = 0.1 m, *WG*

Therefore, we conclude that the locomotion parameters should be adapted to the walking velocity in order to optimize the robot performance. As V_F increases, the values of β and H_B, should be decreased and the value of L_S increased.

Finally, the previous experiences are repeated for the case of the planned robot trajectories. Figure 9 shows the evolution of the locomotion parameters L_S and H_B with V_F when considering the performance index E_{av}. We can see that L_S must increase and H_B must decrease with V_F. These results agree with the previous ones. Regarding the optimal value of β it is independent of V_F, and must be kept small. The variations of the three locomotion parameters (β, L_S, H_B) are similar when analysing the robot locomotion through the other performance indices.

The behaviours just described for the case of a hexapod robot, apply as well to the case of a quadruped robot, either for the different locomotion gaits as for the different controller tunings. These results seem to agree with the observations of the living hexapod and quadruped creatures [11, 12].

C. Gait Selection versus Body Forward Velocity

In a second phase we determine the best locomotion gait, at each forward robot velocity on the range $0.2 \le V_F \le 4.0$ ms^{-1}.

For this purpose, we test the forward straight line quadruped robot locomotion, as a function of V_F, when adopting different gaits often observed in several quadruped animals while they walk / run at variable speeds [7]. Therefore, we consider three walking gaits (Walk, Chelonian Walk and Amble), two symmetrical running gaits (Trot and Pace) and five asymmetrical running gaits (Canter, Transverse Gallop, Rotary Gallop, Half-Bound and Bound). These gaits are usually adopted by animals moving at low, moderate and high speed, respectively.

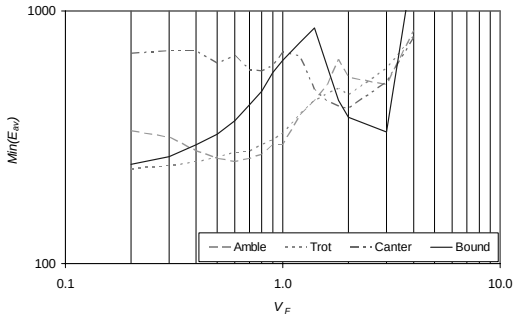

Fig. 10. Plots of min[$E_{av}(V_F)$] for F_C = 0.1 m

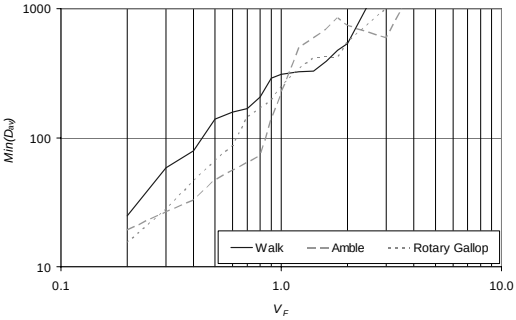

Fig. 11. Plots of min[D_{av} (V_F)] for F_C = 0.1 m

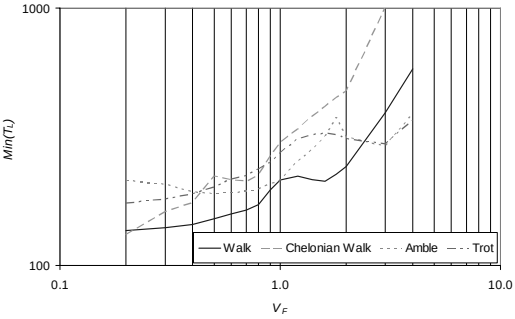

Fig. 12. Plots of min[T_L (V_F)] for F_C = 0.1 m

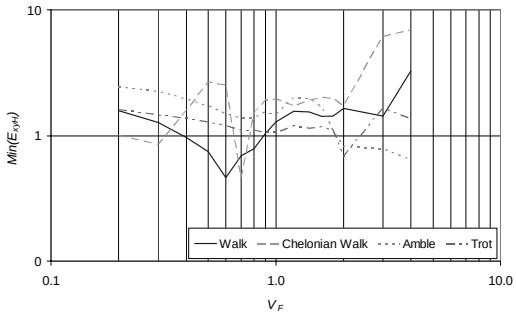

Fig. 13. Plots of min[$\varepsilon_{xyH}(V_F)$] for F_C = 0.1 m

In the analysis are used the system and controller parameters (obtained for the hexapod robot walking with the *WG*, V_F = 1.0 ms^{-1} and β = 50%) presented in Tables I and II, respectively.

Figures 10 – 13 present the charts of min[$E_{av}(V_F)$], min[$D_{av}(V_F)$], min[$T_L(V_F)$] and min[$\varepsilon_{xyH}(V_F)$] for the different gaits. Figure 10 suggests that the locomotion should be Trot, Amble, Canter and Bound as the speed increases. Figure 11 indicates that the Rotary Gallop, Amble and Walk gaits should be adopted for low, medium and high velocities, respectively. Finally, Figures 12 and 13 point out that the quadruped locomotion should adopt Chelonian Walk, Walk, Trot and Amble gaits as V_F increases.

TABLE III

QUADRUPED CONTROLLER PARAMETERS

Gait	Kp_1	Kd_1	Kp_2	Kd_2
Walk	1000	40	2000	40
Chelonian Walk	5000	200	2500	20
Amble	1000	20	1000	60
Trot	1000	140	2000	20
Pace	1000	60	500	40
Canter	1000	0	1500	20
Transverse Gallop	6000	40	1000	40
Rotary Gallop	4000	0	500	80
Half-Bound	4000	0	3000	20
Bound	2000	0	500	20

We can conclude that, from the viewpoint of each proposed optimising index, the robot gait should change with the desired forward body velocity. These results seem to agree with the observations of the living quadruped creatures [12]. However, the results from the different indices are not totally consistent with each other, with exception of T_L and ε_{xyH} (see Fig. 12 and 13).

In order to analyse the influence of the controller tuning, the robot controller is re-tuned for each gait, considering a forward velocity $V_F = 1.0\ \mathrm{ms}^{-1}$ while adopting the locomotion parameters $L_S = 1.0$ m and $H_B = 0.9\ \mathrm{ms}^{-1}$, leading to the controller parameters of Table III.

Fig. 14 analyses the robot locomotion through the index T_L and points out that the quadruped locomotion should adopt the Chelonian Walk, Walk, Amble, Pace and, finally, the Trot gait as the robot speed increases. However, when comparing the results obtained through the other performance indices, we conclude, again, that they are not homogeneous.

Finally, the previous experiences are repeated for the case of the planned robot trajectories. Although not presented here, when analysing the locomotion through the indices E_{av} and T_L the preferred gait is the Bound, on the range of V_F under study. Concerning the analysis through the index D_{av}, the quadruped should adopt the Walk, Amble, Transverse Gallop, Bound and Rotary Gallop gaits as V_F increases. Once again, we conclude that the results obtained through the different performance indices are not homogeneous.

VI. CONCLUSIONS

In this paper we have compared several dynamic aspects of multi-legged robot locomotion gaits. By implementing different motion patterns, we estimated how the robot responds to a variety of locomotion variables such as duty factor, step length and body height and to the forward speed. For analyzing the system performance four quantitative measures were defined based on the system dynamical properties and the trajectory errors. A set of experiments determined the best set of gait and locomotion variables, as a function of the robot velocity.

The results show that the locomotion parameters should be adapted to the walking velocity in order to optimize the robot performance. As the forward velocity increases, the values of β and H_B, should be decreased and the value of L_S increased. Furthermore, for the case of a quadruped robot, we concluded that the gait should be adapted to V_F.

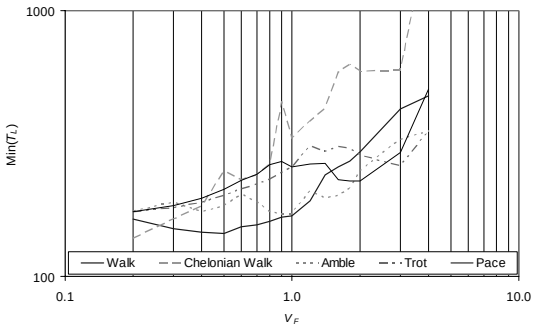

Fig. 14. Plots of min[T_L (V_F)] for F_C = 0.1 m

While our focus has been on a dynamic analysis in periodic gaits, certain aspects of locomotion are not necessarily captured by the proposed measures. Consequently, future work in this area will address the refinement of our models to incorporate more unstructured terrains, namely with distinct trajectory planning concepts. The effect of distinct values of the robot intra-body compliance parameters will also be studied, since animals use their body compliance to store energy at medium and high velocities.

VII. REFERENCES

[1] S.-M. Song and K.J. Waldron, *Machines that Walk: The Adaptive Suspension Vehicle*, MIT Press, 1989.

[2] S. Bai, K. H. Low and T. Zielinska, "Quadruped Free Gait Generation for Straight-Line and Circular Trajectories", *Adv. Rob.*, vol. 13, 1999, pp. 513–538.

[3] D. W. Marhefka and D. E. Orin, "Gait Planning for Energy Efficiency in Walking Machines", in *Proc. of the 1997 IEEE Int. Conf. on Rob. & Aut.*, pp. 474–480.

[4] K. Inagaki, "A Gait Study for a One-Leg-Disabled Hexapod Robot", *Adv. Rob.*, vol. 12, 1999, pp. 593–604.

[5] C.-H. Chen, V. Kumar and Y.-C. Luo, "Motion Planning of Walking Robots Using Ordinal Optimization", *IEEE Rob. & Aut. Mag.*, vol. 5, 1998, pp. 22–32.

[6] S. Bai, K. H. Low and M. Y. Teo, "Path Generation of Walking Machines in 3D Terrain", in *Proc. of the 2002 IEEE Int. Conf. on Rob. & Aut.*, pp. 2216–2221.

[7] http://www.biology.leeds.ac.uk/teaching/3rdyear/Blgy3120/Jmvr/Loco/Gaits/GAITS.htm

[8] M. F. Silva, J. A. T. Machado and A. M. Lopes, "Performance Analysis of Multi-Legged Locomotion Systems", in *Proc. of the 2002 IEEE Int. Conf. on Rob. & Aut.*, pp. 2234–2239.

[9] M. F. Silva, J. A. T. Machado and A. M. Lopes, "Power Analysis of Multi-Legged Systems", in *Proc. b'02 – 15th IFAC World Congress on Aut. Control*, E. F. Camacho, L. Basañez and J. A. de la Puente (eds.).

[10] M. F. Silva, J. A. T. Machado and A. M. Lopes, "Position / Force Control of a Walking Robot", *Machine Intelligence and Robotic Control*, vol. 5, June 2003, pp. 33 – 44.

[11] J. J. Collins and I. Stewart, "Hexapodal Gaits and Coupled Nonlinear Oscillator Models", *Biological Cybernetics*, vol. 68, 1993, pp. 287–298.

[12] R. McN. Alexander, "The Gaits of Bipedal and Quadrupedal Animal", *The Int. J. of Robotics Research*, vol. 3, Summer 1984, pp. 49–59.